Materials and Design 31 (2010) 194–199

Contents lists available at ScienceDirect

Materials and Design

journal homepage: www.elsevier.com/locate/matdes

Characterizing mechanical properties of graphite using molecular dynamics simulation

Jia-Lin Tsai *, Jie-Feng Tu

Department of Mechanical Engineering, National Chiao Tung University, Hsinchu 300, Taiwan

ARTICLE INFO

Article history:
Received 19 March 2009
Accepted 19 June 2009
Available online 23 June 2009

Keywords:
Nano materials (A)
Mechanical (E)
Atomic structure (F)

ABSTRACT

The mechanical properties of graphite in the forms of single graphene layer and graphite flakes (containing several graphene layers) were investigated using molecular dynamics (MD) simulation. The in-plane properties, Young's modulus, Poisson's ratio, and shear modulus, were measured, respectively, by applying axial tensile stress and in-plane shear stress on the simulation box through the modified NPT ensemble. In order to validate the results, the conventional NVT ensemble with the applied uniform strain filed in the simulation box was adopted in the MD simulation. Results indicated that the modified NPT ensemble is capable of characterizing the material properties of atomistic structures with accuracy. In addition, it was found the graphene layers exhibit higher moduli than the graphite flakes; thus, it was suggested that the graphite flakes have to be expanded and exfoliated into numbers of single graphene layers in order to provide better reinforcement effect in nanocomposites.

1. Introduction

With the characteristics of high strength and stiffness, the graphite has been used as reinforcements in composite materials [1]. The natural graphite is constructed by numbers of graphene layers with interlayer spacing of around 3.4 Å. Through chemical oxidation in the environment of sulfuric and nitric acid, the acid intercalant can be intercalated into the graphite galleries to form an intercalated graphite compound. Subsequently, by applying rapid heating because of the vaporization of the acid intercalant in the graphite galleries, the interacted graphite was significantly expanded along the thickness direction and converted into the expanded graphite (EG). After a mechanical mixer together with sonication process, the expanded graphite was dispersed and exfoliated into the polymer matrix to form graphite-reinforced nanocomposites. The synthesizing process for manufacturing the nanocomposites was discussed in detail in the literatures [2,3]. Recently, Si and Samulski [4] employed platinum nanoparticles adhered to the graphene to prevent the aggregation of isolated graphene sheets during the drying process. However, the stacked graphene structures (so called graphite flakes) are commonly observed in TEM micrographs and XRD examination [5], and it is a challenging task to fully exfoliate the aggregated graphene sheets. In fact, graphite flakes together with graphene layers are commonly observed in graphite nanocomposites and it is important to clarify if the two atomistic configurations of the graphite, i.e., graphite flakes and single graphene layer, would have the same mechanical properties. Moreover, in order to accurately characterize the mechanical properties of the graphite-reinforced nanocomposites, an exploration of the fundamental properties of the graphite associated with different microstructures is required.

Cho et al. [6] performed a molecular structural analysis to calculate the graphite's elastic constants. The in-plane properties of graphite were derived by considering the geometric deformation of a single graphene sheet subjected to in-plane loading. However, for the out-of-plane properties, they modeled the graphic as graphic flake with multi graphene layers, the non-bonded atomistic interactions of which were described using Lennard-Jones potential function. Scarpa et al. [7] proposed truss-type analytical models in conjunction with cellular material mechanics theory to describe the in-plane elastic properties of single layer graphene sheets. It was found that the analytical results and the numerical results obtained from finite element shows good agreement with existing numerical values. Hemmasizadeh et al. [8] who correlated the force-depth results obtained from MD simulation with the large deflection formulation of circular plates loaded at center to evaluate the effective Young's modulus of graphene sheet and the corresponding wall thickness of the single sheet. By using MD simulation, Bao et al. [9] investigated the variations of Young's modulus of graphite, which contains different numbers of graphene layers (one to five layers). Results indicated that there is no considerable difference in Young's modulus between the single layer of graphene and graphite flakes with five layers of graphene. Reddy et al. [10] modeled the elastic properties of a finite-sized graphene sheet using continuum mechanics approach based on

* Corresponding author. Tel.: +886 3 5731608; fax: +886 3 5720634.
E-mail address: jialin@mail.nctu.edu.tw (J.-L. Tsai).

0261-3069/$ - see front matter © 2009 Elsevier Ltd. All rights reserved.
doi:10.1016/j.matdes.2009.06.032

Brenner's potential [11]. The computed elastic constants of the graphene sheet are found to follow the orthotropic material behaviors. In addition to the fundamental material properties, the vibrational responses of single layer graphene sheets were investigated through a molecular structural mechanics approach [12]. Both mode shapes and natural frequency of single graphene sheet were considered in their analysis. In light of the forgoing, most studies characterize the elastic properties of the graphite based on the behavior of a single graphene sheet; the mutual influences of the adjacent graphene layers on the mechanical responses in the graphite flakes are rarely taken into account. As previously mentioned, both the graphene layer and the graphite flakes were commonly found in the nanocomposites, so it is not adequate to utilize the properties of the graphene sheet instead of the graphite flakes in the modeling of graphite-reinforced nanocomposites.

In this study, the mechanical properties of the graphite flakes and the graphene were systematically characterized using MD simulation. Both bonded and non-bonded interactions were accounted for in the description of the atomistic graphite structures. By applying uniaxial tensile loading on the atomistic graphite structures, the Young's modulus and Poisson's ratio were determined from the strain field in the deformed configuration. In the same manner, the shear modulus was predicted from the shear deformation associated with the applied shear stress. The properties of the single graphene layer were then compared to those of the graphite flakes with multi-layers of graphene.

2. Molecular dynamics simulation

2.1. Construction of atomistic structures of graphite

Graphite structure is constructed by the carbon layers where the carbon atoms are arranged in a hexagonal pattern. The interatomistic distance between the adjacent carbon atoms is 1.42 Å, and the associated atomistic interaction is covalently bonded by sp^2 hybridized electrons, the bond angle of which is 120° to each other. In naturally occurring or high quality synthetic graphite, the carbon layers are attacked along the thickness direction in AB type sequence with interlayer spacing of approximately 3.4 Å as shown in Fig. 1. Hereafter, the graphite with several carbon layers lumped together is referred to as graphite flakes. Because the adjacent carbon layers are held together by the weak van der Waals force, after proper processing [2,3], the stacked carbon layers can be dispersed and separated into a single layer that is usually called graphene sheet or graphene layer.

In order to investigate the mechanical properties of the graphite flakes and the graphene layer, the atomistic structures have to be constructed in conjunction with the appropriately specified atomistic interaction. In the description of graphite structure, two kinds of atomistic interactions are normally taken in account; one is bonded interaction, such as the covalent bond, and the other is the non-bonded interaction, i.e., van der Waals and electrostatic forces. Among the atomistic interactions, the covalent bond between two neighboring carbon atoms that provides the building block of the primary structure of the graphite may play an essential role in the mechanical responses. Such bonded interaction can be described using the potential energy that consists of bond stretching, bond angle bending, torsion, and inversion as illustrated in Fig. 2 [13]. Therefore, the total potential energy of the graphite contributed from the covalent bond is given as

$$U_{\text{graphite}} = \sum U_r + \sum U_\theta + \sum U_\phi + \sum U_\omega \tag{1}$$

where U_r is a bond stretching potential; U_θ is a bond angle bending potential; U_ϕ is a dihedral angle torsional potential; and U_ω is an inversion potential. For graphite structures under in-plane deformation, the atomistic interaction is mainly governed by the bond stretching and bond angle bending therefore, the dihedral torsion and inversion potentials that are related to the out-of-plane deformation were disregarded in the modeling. The explicit form for the bond stretching and bond angle bending can be approximated in terms of elastic springs as [14]:

$$U_r = \frac{1}{2}k_r(r - r_0)^2 \tag{2}$$

$$U_\theta = \frac{1}{2}k_\theta(\theta - \theta_0)^2 \tag{3}$$

where k_r and k_θ are the bond stretching force constant and angle bending force constant, respectively. The constants $k_r = 93,800\ \frac{\text{kcal}}{\text{mole nm}^2}$ and $k_\theta = 126\ \frac{\text{kcal}}{\text{mole rad}^2}$ selected from AMBER force field for carbon–carbon atomic-interaction [15] was employed in our molecular simulation. The parameters r_0 and θ_0 represent bond length and bond angle in equilibrium position, which are assumed to be 1.42 Å and 120°, respectively, for the graphite atomistic structures.

In addition to the bonded interaction, the non-bonded interaction between the carbon atoms was regarded as the van der Waals force, which can be characterized using the Lennard-Jones (L-J) potential as

$$U_{vdW} = 4u\left[\left(\frac{r_0}{r_{ij}}\right)^{12} - \left(\frac{r_0}{r_{ij}}\right)^{6}\right] \tag{4}$$

where r_{ij} is the distance between the non-bonded pair of atoms. For the hexagonal graphite, the parameters $u = 0.0556$ kcal/mole and $r_0 = 3.40$ Å suggested in the literature [16] were adopted in the modeling. Moreover, the cutoff distance for the van der Waals force

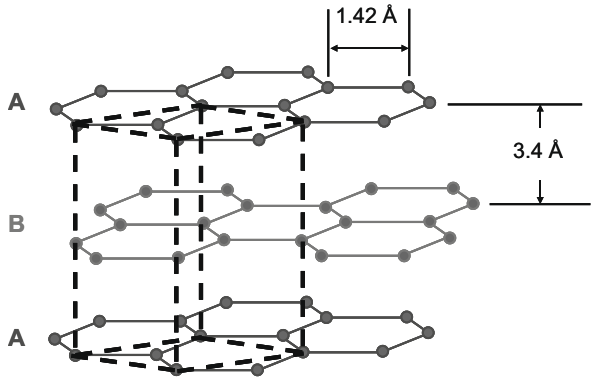

Fig. 1. Schematic of graphite structures.

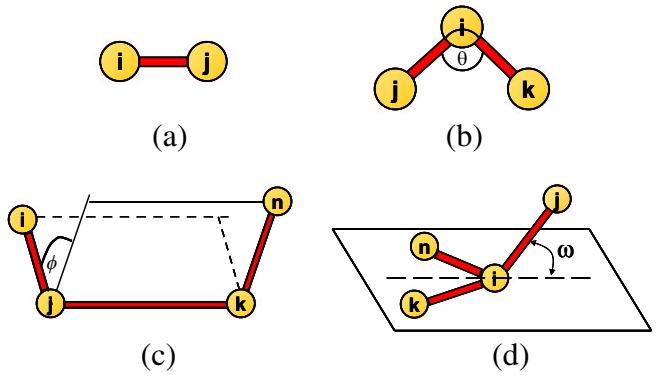

Fig. 2. A schematic of the inter-atomic potential: (a) bond stretch; (b) bond angle bending; (c) dihedral angle torsion; (d) inversion

is assigned to be 10 Å, which means that beyond this distance, there are no more van der Waals interactions taking place.

In order to model the material properties of graphite flakes and the graphene sheet, the simulation box suitable for representing the corresponding atomistic structures has to be established. Fig. 3 shows the schematic of the simulation box for graphite flakes and the graphene sheet as well. A periodic boundary condition was implemented on all surfaces to demonstrate the infinite graphite structures. It is noted in the graphene sheet that the dimension of the simulation box in the thickness direction is set to be large enough that the van der Waals interaction between the neighboring layers can not be attained. This especial design of the simulation box is intended to simulate the exfoliated graphene sheets. The atomistic structures with stress-free configuration were obtained by performing an NPT ensemble with time increments at 1 fs for 100 ps (the total iteration steps are 100,000) until the potential energy accomplished a stable value. The NPT ensemble represents that the pressure and temperature of the system may approach to the specified values during the MD simulation. This process is accomplished through the Berendsen thermostat [17,18] by scaling the velocities and positions of atoms at each step to push the temperature and pressure toward the desired value ($P = 0$ and $T = 0$ K). Figs. 4 and 5 demonstrate the potential energy history and the temperature variation, respectively, for the graphene sheet during the NPT ensemble. It seems that the potential energy attains a stable value rapidly, and the temperature also approaches to 0 K. Based on the observations, it was suggested that the current atomistic structure is in the equilibrium condition and suitable for the characterization of the material properties. The MD simulation was carried out under the DL-POLY package originally developed by Daresbury Laboratory [19] in conjunction with the homemade subroutine for post-processing.

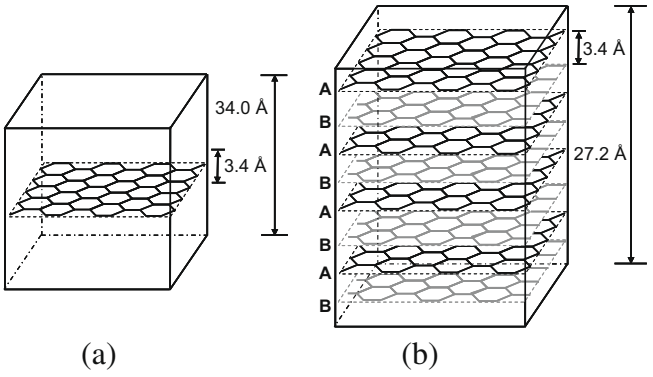

Fig. 3. Schematic of atomistic model in the MD simulation for: (a) graphene sheet and (b) graphite flakes.

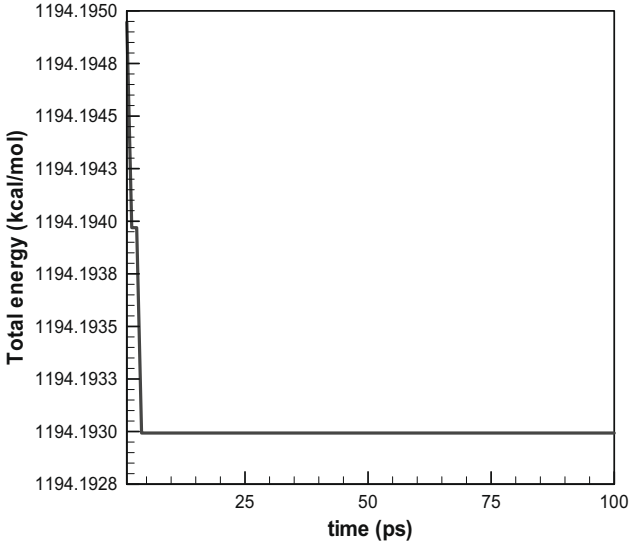

Fig. 4. Variation of potential energy in the modified NPT ensemble for a graphene sheet.

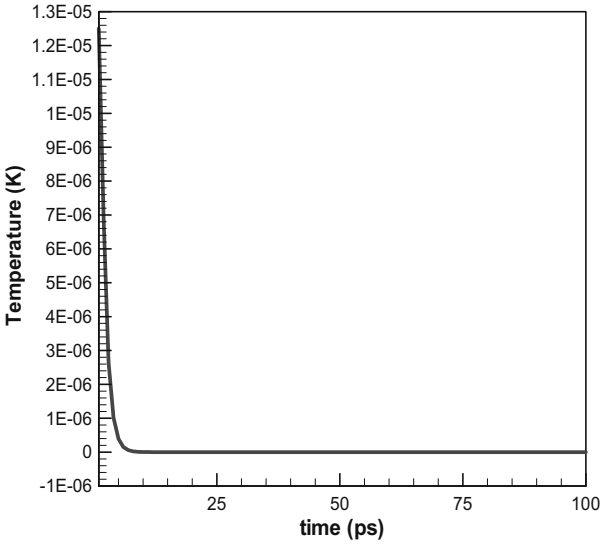

Fig. 5. Variation of temperature in the modified NPT ensemble for a graphene sheet.

2.2. Characterizing the Young's modulus and Poisson's ratio of the graphite

The methodology developed to evaluate the mechanical properties of the atomistic structures was motivated from the technique commonly used in the continuum solid. For continuum solids, the Young's modulus and Poisson's ratio are measured from the simple tension test. The same concept was extended and applied to the atomistic structures by means of a modified NPT ensemble in MD simulation with the characteristics of varying a simulation box in shape and size [20]. In other words, axial stresses can be implemented on both sides of the simulation box with other faces' being traction free as shown in Fig. 6. Again, after the energy minimization process, the equilibrated graphite atomistic structure under axial loading was obtained, and the Young's modulus and Poisson's ratio was defined in the continuum manner as

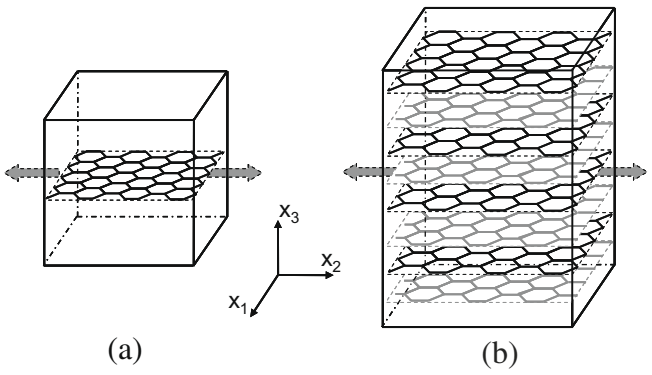

Fig. 6. Axial stress applied in: (a) graphene sheet and (b) graphite flakes.

$$E = \frac{\sigma}{\varepsilon_1} \tag{5}$$

$$v_{12} = -\frac{\varepsilon_2}{\varepsilon_1} \tag{6}$$

where ε_1 is the strain component measured in the loading direction, and ε_2 is the strain component measured in the lateral direction. As is noted in Eq. (5), σ should be the stress directly acting on the graphite structure. However, for the case of graphene sheet as shown in Fig. 6a, because the dimension of the graphene sheet in thickness direction is not compatible to the size of the simulation box, the stress in the graphene sheet has to be converted from the stress acting on the simulation box, σ_{box}, in terms of the geometric parameters as

$$\sigma = \frac{\sigma_{box} h}{t} \tag{7}$$

where h is the height of the simulation box, and t is the thickness of the graphene sheet, which is equal to 3.4 Å. The Young's modulus and Poisson's ratio obtained from MD simulation for the graphite flakes and graphene sheet are presented, respectively, in Table 1.

Instead of the application of axial stress, the graphite properties can be calculated alternatively by applying a small amount of strain on the simulation box with the other strain components remaining at zero. Because this approach is commonly employed in MD simulation to determine the Young's modulus of atomistic structures [21–23], it was utilized to verify the results presented in the previous section. When the graphite in the stress-free state was obtained through MD simulation, a small amount of axial strain component was applied on the simulation box while the other strain components remain at zero as shown in Fig. 7. After an energy minimization process in the NVT ensemble where the volume and temperature are fixed during the simulation, the associated stress in the deformed configuration of the atomistic structure was calculated through the virial theorem [18] as

$$\sigma_{ij} = -\frac{1}{V_0}\left(\sum_{i<j} r_{ij} f_{ij}^T\right) \tag{8}$$

In Eq. (8), r_{ij} and f_{ij} denotes the atomic distance and the corresponding interaction force between any two atoms. V_o represents the total volume of the simulation box. In the same manner, the stress component on the simulation box has to be converted into the one on the graphene sheet by using Eq. (7). It is noted that in Eq. (8), because the atomistic model was simulated at 0 K, the velocity term caused by temperature was neglected in the stress computation. For the graphite layer structures, the constitutive relation under plane stress assumption can be written in terms of the stiffness matrix C_{ij} as

$$\begin{Bmatrix} \sigma_{11} \\ \sigma_{22} \\ \tau_{12} \end{Bmatrix} = \begin{bmatrix} C_{11} & C_{12} & 0 \\ C_{21} & C_{22} & 0 \\ 0 & 0 & C_{66} \end{bmatrix} \begin{Bmatrix} \varepsilon_{11} \\ \varepsilon_{22} \\ \gamma_{12} \end{Bmatrix} \tag{9}$$

and the values of the entries in the C_{ij} matrix can be calculated from the measured stress components corresponding to the applied strain filed in the NVT ensemble. Once the values were determined, the Young's modulus and Poisson's ratio of the graphite can be deduced as [24]

$$E = \frac{C_{11}C_{22} - C_{12}C_{21}}{C_{22}} \tag{10}$$

$$v_{12} = \frac{C_{12}}{C_{22}} \tag{11}$$

Table 2 shows the values of the elements in the stiffness matrix with regard to the applied strain of 0.001. In addition, the calculated modulus and Poisson's ratio are also included in the same table. It was found that the modulus and Poisson's ratio derived based on Eqs. (10) and (11) are in agreement with the predictions obtained

Table 1
Comparison of in-plane elastic constants of graphite flakes and graphene sheet obtained from the modified NPT ensemble.

	E (TPa)	v	G_{12} (TPa)
Graphene	0.912	0.261	0.358
Graphite flakes	0.795	0.272	0.318

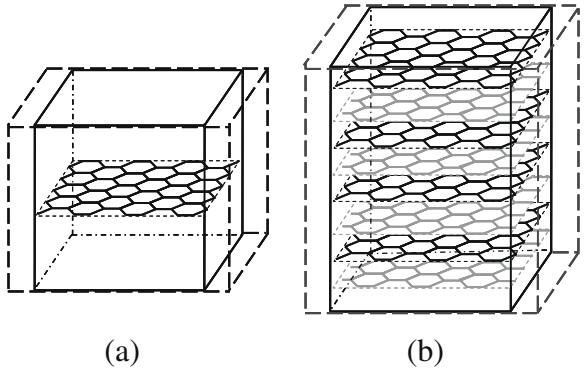

Fig. 7. Axial deformation applied in: (a) graphene sheet and (b) graphite flakes (the solid line denotes the undeformed configuration and the dashed line indicates the deformed shape).

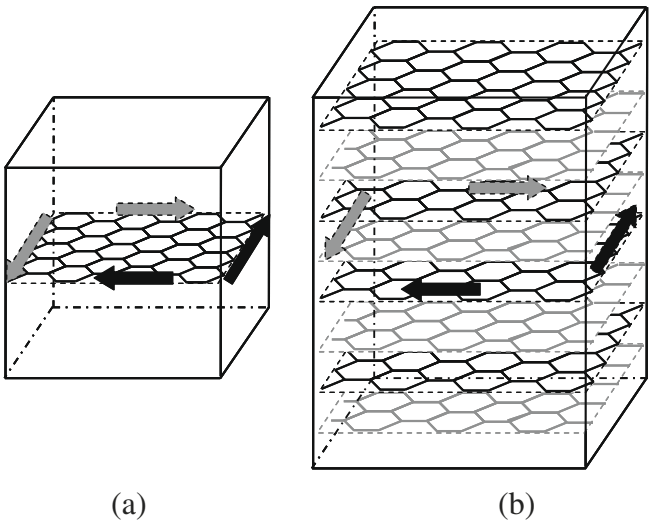

Fig. 8. In-plane shear stress applied in: (a) graphene sheet and (b) graphite flakes.

Table 2
The elements in the stiffness matrix for the graphene sheet and graphite flakes calculated based on axial strain deformation in conventional NVT ensemble.

	C_{11} (GPa)	C_{12} (GPa)	C_{21} (GPa)	C_{22} (GPa)	E (TPa)	v
Graphene	977.91	254.46	254.74	978.19	0.912	0.26
Graphite flakes	864.29	235.16	235.21	864.34	0.8	0.272

Table 3
Comparison of the predicted values with others listed in the literatures.

	Graphene	Graphite flakes	Cho et al. [6]	Bao et al. [9]	Reddy et al. [10]	Blakslee [25]
E (TPa)	0.912	0.795	1.153	1.026	0.671	1.020
v	0.261	0.272	0.195	–	0.428	0.160
G_{12} (TPa)	0.358	0.318	0.482	–	0.384	0.440

from the uniaxial stress method. This conformity clearly reveals that the modified NPT ensemble with the technique of applied loading is suitable for characterizing material properties of the atomistic structure. In the next section, the modified NPT ensemble will be adopted to characterize the shear modulus of the graphite with respect to the applied shear loading.

2.3. Characterization of shear modulus G_{12}

By following the same technique used in the early section, the shear modulus of the atomistic structure can be evaluated via the application of in-plane shear stress on the simulation box as shown in Fig. 8. This process is accomplished by conducting the modified NPT ensemble in MD simulation. After the energy minimization process, the deformed configuration of the simulation box was calculated from which the shear strain associated with the applied shear stress was determined. If the deformation is small, the shear modulus of the graphite can be defined based on the theory of linear elasticity as

$$G = \frac{\tau}{\gamma} \tag{12}$$

where τ is the applied shear stress, and γ is the corresponding shear strain determined from MD simulation. The shear moduli calculated with Eq. (12) for the graphite flakes and graphene sheet are also listed in Table 1.

3. Results and discussion

Results presented in Table 1 indicate that the single graphene sheet demonstrates higher Young's modulus and shear modulus than the graphite flakes. Thus, it was suggested that to achieve better mechanical properties of nanocomposites, the aggregated graphite flakes need to be exfoliated in the form of graphene sheets and uniformly dispersed into the matrix systems. Moreover, according to the relationship between Young's modulus, shear modulus, and Poisson's ratio, it was found that both graphite flakes and graphene demonstrate isotropic in-plane properties. This isotropic property could be attributed to the hexagonal array of the carbon atoms.

For the purposes of comparing, the calculated material properties of the graphite are listed together with other published predictions in Table 3. It was revealed that the moduli obtained from the current model are a little less than those listed in the literature although the discrepancy is not much. This difference could be resulting from the different potential functions employed in the modeling of the atomistic interaction of the carbon atoms. On the other hand, it should be indicated that most of the published values are calculated based on the graphene sheet except the one addressed by Bao et al. [9] who investigated the Young's modulus of graphite with numbers of graphene layers (from one layer up to five layers). In their investigation, there is no significant difference in Young's modulus between the single graphene layer and the graphite flake with five-layer graphene. It is possible that the dissimilarity may not be considerable just by comparing the single layer graphene with the five-layer graphene. On the contrary, our prediction considers the periodic boundary condition in the thickness direction and would be close to the behavior of the graphite flakes with numbers of graphene layers. This is the reason why in our simulation, the graphic flakes would exhibit different material properties from the single graphene sheet. In addition, for the sake of comparison, the experimental values for the graphite structures provided by Blakslee et al. [25] were added in Table 3. It shows that the values predicted based on the graphene sheet model have a better agreement with the experimental data.

4. Conclusions

The in-plane properties of graphene sheet and the graphite flakes were investigated using MD simulation. Two approaches were introduced to calculate the Young's modulus and Poisson's ratio: one is the applied axial stress on the simulation box under the modified NPT ensemble, and the other is the applied axial strain on the simulation box through the NVT ensemble. The values calculated based on the two approaches have good agreement with each other, and the modified NPT ensemble, similar to the continuum mechanics approach, was regarded as an effective way to characterize the material properties of atomistic structures. Furthermore, the shear modulus was evaluated by taking the ratio of the applied in-plane shear stress to the corresponding shear strain. Because of the hexagonal array of the carbon atoms, the in-plane shear modulus, Young's modulus, and Poisson's ratio of the graphite flakes and graphene sheet satisfy the isotropic properties. A comparison of in-plane properties of the graphene sheet and graphite flakes reveals that the single graphene sheet exhibits higher modulus than the graphite flakes; therefore, the exfoliation of the graphite flakes into graphene layers is essential in order to have better mechanical properties of graphite-reinforced nanocomposites.

References

[1] Fukushima H, Drzal LT. Graphite nanoplatelets as reinforcements for polymers: structural and electrical properties. In: Proceedings of the American society for composites, The 17th technical conference; October 2002. p. 21–23.
[2] Li J, Kim JK, Sham ML. Conductive graphite nanoplatelet/epoxy nanocomposites: effect of exfoliation and UV/ozone treatment of graphite. Scripta Mater 2005;53:235–40.
[3] Fukushima H, Drzal LT, Rook BP, Rich MJ. Thermal Conductivity of Exfoliated Graphite Nanocomposites. J Therm Anal Calorim 2006;85(1):235–8.
[4] Si Y, Samulski ET. Exfoliated graphene separated by platinum nanoparticles. Chem Mater 2008;20:6792–7.
[5] Yasmin A, Luo JJ, Daniel IM. Processing of expanded graphite reinforced polymer nanocomposites. Compos Sci Technol 2006;66:1182–9.
[6] Cho J, Luo JJ, Daniel IM. Mechanical characterization of graphite/epoxy nanocomposites by multi-scale analysis. Compos Sci Technol 2007;67:2399–407.
[7] Scarpa F, Adhikari S, Phani AS. Effective elastic mechanical properties of single layer graphene sheets. Nanotechnology 2009;20:065709.
[8] Hemmasizadeh A, Mahzoon M, Hadi E, Khandan R. A method for developing the equivalent continuum model of a single layer graphene sheet. Thin Solid Films 2008;516:7636–40.
[9] Bao WX, Zhu CC, Cui WZ. Simulation of Young's Modulus of single-walled carbon nanotubes by molecular dynamics. Physica B 2004;352:156–63.
[10] Reddy CD, Rajendran S, Liew KM. Equilibrium configuration and continuum elastic properties of finite sized graphene. Nanotechnology 2006;17:864–70.
[11] Brenner DW. Empirical potential for hydrocarbons for use simulating the chemical vapor deposition of diamond films. Phys Rev B 1990;42(15):9458–71.
[12] Sakhaee-Pour A, Ahmadian MT, Naghdabadi R. Vibrational analysis of single-layered graphene sheets. Nanotechnology 2008;19:085702.
[13] Rappe AK, Casewit CJ. Molecular mechanics across chemistry. Sausalito (CA): University Science Books; 1997.

[14] Li C, Chou TW. A structural mechanics approach for the analysis of carbon nanotubes. Int J Solids Struct 2003;40(10):2487–99.
[15] Cornell WD, Cieplak P, Bayly CI, Gould IR, Merz Jr KM, Ferguson DM, et al. A second generation force field for the simulation of proteins, nucleic acids, and organic molecules. J Am Chem Soc 1995;117(19):5179–97.
[16] Battezzatti L, Pisani C, Ricca F. Equilibrium conformation and surface motion of hydrocarbon moleculars physisorbed on graphite. J Chem Soc 1975;71: 1629–39.
[17] Berendsen HJC, Postma JPM, van Gunsteren WF, DiNola A, Haak JR. Molecular dynamics with coupling to an external bath. J Chem Phys 1984;81(8): 3684–90.
[18] Allen MP, Tildesley DJ. Computer simulation of liquids. Oxford: Clarendon Press; 1990.
[19] Smith W, Forester TR. The DL_POLY user manual, version 2.13. Daresbury (Warrington, England): Daresbury Laboratory, CCLRC; 2001.
[20] Melchionna S, Ciccotti G, Holian BL. Hoover NPT dynamics for systems varying in shape and size. Mol Phys 1993;78(3):533–44.
[21] Agrawal PM, Sudalayandi BS, Raff LM, Komanduri R. A comparison of different method of Young's Modulus determination for single-wall carbon nanotubes (SWCNT) using molecular dynamics (MD) simulations. Comput Mater Sci 2006;38:271–81.
[22] Suzuki K, Nomura S. On elastic properties of single-walled carbon nanotubes as composite reinforcing fillers. J Compos Mater 2007;41(9): 1123–35.
[23] Adnan A, Sun CT, Mahfuz H. A molecular dynamics simulation study to investigate the effect of filler size on elastic properties of polymer nanocomposites. Compos Sci Technol 2007;67(3–4):348–56.
[24] Gere JM. Mechanics of materials. Cheltenham (UK): Nelson Thornes; 2001.
[25] Blakslee OL, Proctor DG, Seldin EJ, Spence GB, Weng T. Elastic constants of compression-annealed pyrolytic graphite. J Appl Phys 1970;41:3373–82.